

# From Sim-to-Real: Toward General Event-based Low-light Frame Interpolation with Per-scene Optimization

Ziran Zhang<sup>1,2\*</sup>, Yongrui Ma<sup>3,2\*</sup>, Yueting Chen<sup>1</sup>, Feng Zhang<sup>2</sup>, Jinwei Gu<sup>3</sup>, Tianfan Xue<sup>3†</sup>, Shi Guo<sup>2†</sup>

<sup>1</sup>Zhejiang University, Hangzhou, China    <sup>2</sup>Shanghai AI Laboratory, Shanghai, China

<sup>3</sup>The Chinese University of Hong Kong, Hong Kong, China

naturezhanghn@zju.edu.cn, yongrayma@gmail.com, chenyt@zju.edu.cn, zhangfeng@pjlab.org.cn,  
jwgu@cse.cuhk.edu.hk, tfxue@ie.cuhk.edu.hk, guoshi@pjlab.org.cn

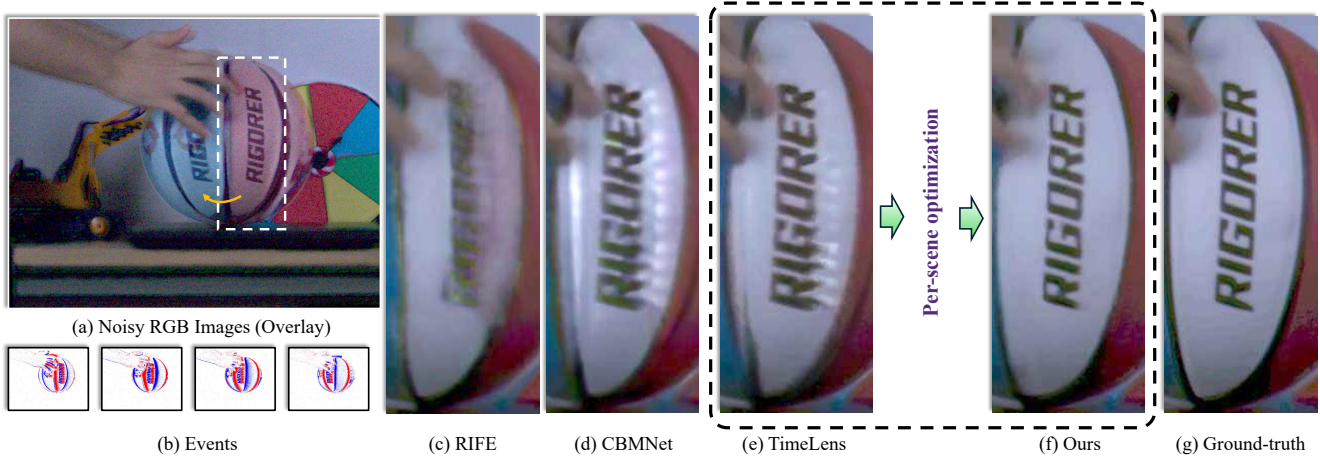


Figure 1. The interpolated result from the real-captured RGB-Event sequence under low light conditions. Our proposed per-scene optimization method can successfully correct the impact of event latency, accurately interpolate the correct positions, and produce visually pleasing interpolation results.

## Abstract

Video Frame Interpolation (VFI) is important for video enhancement, frame rate up-conversion, and slow-motion generation. The introduction of event cameras, which capture per-pixel brightness changes asynchronously, has significantly enhanced VFI capabilities, particularly for high-speed, nonlinear motions. However, these event-based methods encounter challenges in low-light conditions, notably trailing artifacts and signal latency, which hinder their direct applicability and generalization. Addressing these issues, we propose a novel per-scene optimization strategy tailored for low-light conditions. This approach utilizes the internal statistics of a sequence to handle degraded event data under low-light conditions, improving the generalizability to different lighting and camera settings. To evaluate its robustness in low-light condition, we further introduce EVFI-LL, a unique RGB+Event dataset captured under low-light conditions. Our results

\* Authors contributed equally

† Corresponding author

demonstrate state-of-the-art performance in low-light environments. Both the dataset and the source code will be made publicly available upon publication. Project page: <https://naturezhanghn.github.io/sim2real>.

## 1. Introduction

Video frame interpolation (VFI) has extensive applications in video enhancement, frame rate up-conversion, and slow-motion generation. The advent of event cameras [2, 24] has demonstrated a good potential for VFI, because it can asynchronously capture of per-pixel brightness changes with much higher temporal resolution and higher dynamic range. Recent studies [11, 28–30] have explored the event-based video frame interpolation (Event-VFI), demonstrating significant performance enhancements compared to the traditional RGB-based VFI [1, 7, 26].

However, the performance of Event-VFI degrades in low light captures due to the noticeable trailing artifacts associated with event signals [15, 17, 20]. As shown in Fig. 1 (d) and (e), one can observe that in the results from the cur-

rent Event-VFI methods, such as TimeLens [30] and CBM-Net [11], there is noticeable ghosting of letters due to event latency, and the interpolated frames exhibit noticeable trailing artifacts. Given that low light conditions are common, investigating Event-VFI under low light conditions represents a meaningful and practical yet challenging task.

The low-light condition presents another challenge to Event-VFI: the latency, noise, and other degradations in the event signals are not easy to model. One line of solution [13, 14, 34] is to simulate more realistic events by accounting for various degradation factors, including leak noise events, refractory periods, and shot noise, using event simulators, such as v2e [6] or ESIM [21]. However, even with an improved simulation pipeline, a significant discrepancy between simulated data and real-world data still exists [17]. Another solution [17] focuses on collecting real-world event datasets to bridge the gap between simulated and actual event signals. However, dataset acquisition is costly, and the datasets tailored to one particular camera with a fixed setting cannot generalize to other cameras or even to other settings. Thus, this raises an interesting and challenging question: *how can the Event-VFI method be cost-effectively generalized to real-world low-light conditions with varying camera settings?*

To address the above question, we propose a novel per-scene optimization strategy for general Event-VFI in low light conditions. Because the trailing artifacts and other degradations in event signals are hard to model at the training stage, we instead perform per-scene optimization to adapt an interpolation model to a specific distribution of that event stream. This is based on the insight that these degradations are mostly influenced by illuminance, camera hardware, and capture settings, which are relatively constant in a single video. As shown in Fig. 2, unlike previous Event-VFI methods [11, 29, 30], our method first utilizes the entire input sequence to fine-tune a pre-trained Event-VFI model. Specifically, we use the captured RGB image  $I_t$  at time  $t$  as the ground truth (with denoising applied) to supervise the interpolation results from two other captured RGB frames ( $I_{t-1}$  and  $I_{t+1}$ ) at neighboring timestamps and event signals ( $E_{t-1,t}$  and  $E_{t,t+1}$ ) during this interval. Then, at the actual inference stage, the fine-tuned network is applied to the same sequence to generate a novel frame  $\hat{I}_{t+\Delta t}$  to actually increase the frame rate.

Additionally, we also improve the robustness of pre-trained Event-VFI in low-light conditions. We revisit and refine the low-light event modeling process [4, 5, 17, 20, 22], carefully designing a simulation pipeline tailored for low-light Event-VFI. Utilizing our pre-trained model, our per-scene optimized approach achieves state-of-the-art performance in processing real-world low-light sequences. Additionally, the running time for per-scene optimization is comparable to that of the inference process, thereby ensur-

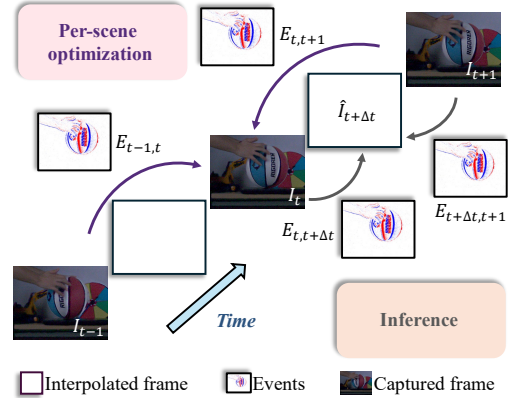


Figure 2. Illustration of the proposed per-scene optimization process.

ing that these improvements are achieved at minimal cost.

To evaluate the proposed solution, we also developed EVFI-LL, a novel RGB-Event interpolation benchmark designed for low-light. Unlike previous datasets captured at normal lighting conditions, such as BS-ERGB [30] and ERF-X170FPS [11], EVFI-LL consists of sequences captured under low-light conditions under 35 Lux. Notably, EVFI-LL is the first dataset to capture events using different ON/OFF thresholds (three settings: -20, 0 [default], and 20) on the Prophesee EVK4-HD event sensor. Comprising over 20 testing sequences, this dataset includes accurately synchronized RGB videos and event streams, establishing a new benchmark for evaluating low-light Event-VFI. Additionally, it allows for an assessment of the generalizability of Event-VFI methods across various ON/OFF thresholds. Both the code and dataset will be made publicly available upon publication.

## 2. Related Work

### 2.1. RGB-based Video Frame Interpolation

Video frame interpolation is a fundamental and challenging task that aims to generate inter-frames between consecutive frames in a video. Typical solutions for RGB-based video frame interpolation (RGB-VFI) can be classified into flow-free and flow-based methods. For the flow-free methods, the interpolated frame is generated directly from input frames without explicit flow estimation [18, 19, 25]. [19] utilized adaptive separable convolution for interpolation, achieved trained end-to-end using widely available video data without any human annotation. PhaseNet [18] estimated the phase decomposition of the intermediate frame. [25] proposed a Transformer-based interpolation strategy that reduces memory consumption and improves efficiency through local attention and a space-time separation strategy.

For the Flow-based methods [1, 7, 26], the flow is explic-

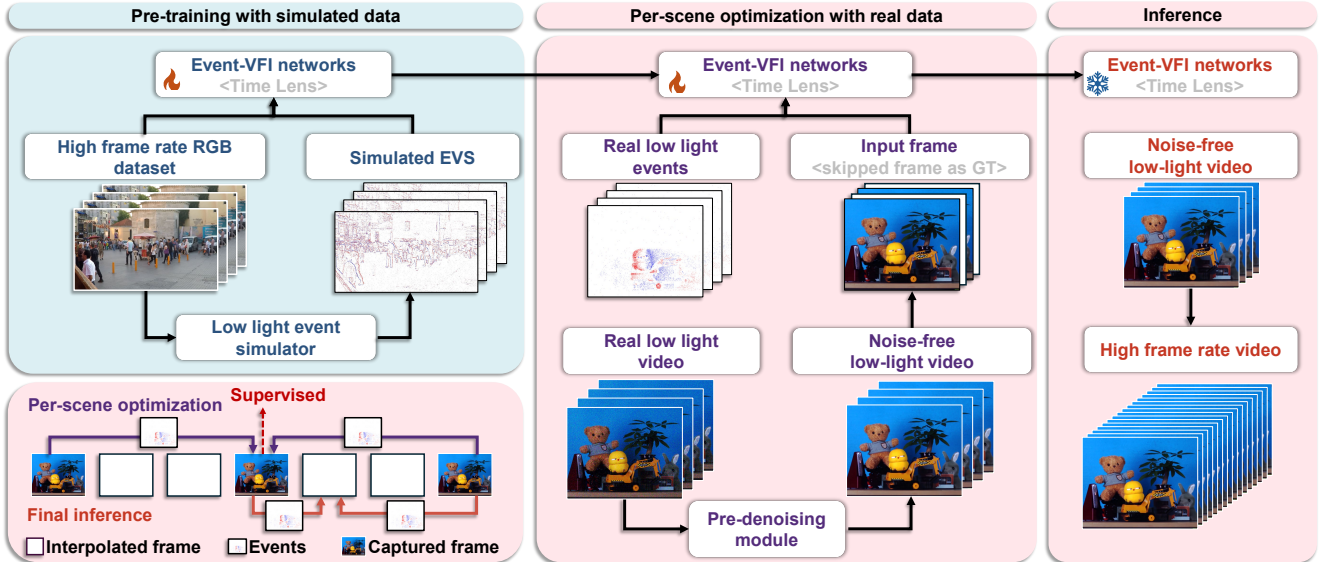


Figure 3. Overview of the proposed low light Event-VFI method. This framework encompasses the pre-training phase, per-scene optimization, and inference process.

itly estimated in the interpolation. [1] developed a depth-aware flow projection layer to synthesize intermediate flows that preferably sample closer objects than farther ones. [26] proposed bidirectional optical flow learning for interpolating large motions and complex textures. [7] introduced RIFE, which can estimate the intermediate flows end-to-end with much faster speed. However, due to a lack of accurate motion information between two RGB frames, the performance of RGB-VFI degrades when handling complex and large motion.

## 2.2. Event-based Video Frame Interpolation

Event cameras record intensity changes of objects, offering high frame rate and high dynamic range characteristics [15, 20], which is benefit for VFI task. Thus, using event cameras for VFI (Event-VFI) has recently provided a new direction for addressing non-linear, large motion interpolation [11, 28–30]. Time Lens [30] and Time Lens++ [29] demonstrated promising performance in non-linear motion scenarios. [28] proposed REFID, which jointly performs image deblurring and interpolation. [11] introduced CBM-Net for interpolation with cross-modal asymmetric bidirectional motion field estimation.

Even though Event-VFI methods exhibit better performance in handling non-linear motions, current research has not addressed Event-VFI task in low-light conditions. In low light, event cameras produce noticeable trailing artifacts [15, 17, 20], which negatively impact event-based interpolation. Thus in this paper, we study this promising yet under-explored low light Event-VFI problem.

## 2.3. Low-light Event Correction

In low light, event cameras produce noticeable trailing artifacts and noise [15, 17, 20] which degrade the follow-up tasks. To correct these degradation in low-light events, some methods [14, 34] utilize more realistic event simulation. Specially, [14, 34] utilized the commonly used v2e [6] or ESIM [21] simulator, and considered various degradation factors such as threshold noise, hot pixels, leak noise events, refractory period, and shot noise. However, event signal generated by such simulation method still has great gap with real-captured data and the model trained with simulated data can not directly generalize to real-world events and correct the trailing artifacts of low light events [17].

To correct the real-world latency and noise of event signal, [17] collected a real-world low-light event dataset consisting of low-light events and high-quality images. A learnable event timestamps calibration model is also proposed to learn the event trailing. However, such method needs costly data collection. More importantly, such methods [17] mainly focusing on correct event signal for specific event camera, specifically for Prophesee EVK4, with fixed camera setting, *e.g.*, ON/OFF thresholds. However, the hardware differences and parametric setting both effect the latency degree, limiting their generalization. To solve these limitations, in this paper, a per-scene optimization strategy is proposed for low light Event-VFI task to let our model can generalize to event camera with different camera setting without costly data collection.

### 3. Problem definition

#### 3.1. Low-light Event Representation

Event camera capture scene illumination change as an asynchronous stream of events. Each event at position  $\mathbf{u} = (x, y)$  is generated when the intensity change is larger than a contrast threshold  $c$ : [11, 29, 30]:

$$E_t = \begin{cases} 1, & \text{if } \log(I_t) - \log(I_{t-\Delta t}) \geq c, \\ -1, & \text{if } \log(I_t) - \log(I_{t-\Delta t}) \leq -c, \\ 0, & \text{otherwise,} \end{cases} \quad (1)$$

where  $E_t$  and  $I_t$  are the event polarity and the image intensity at time  $t$ , respectively, and  $\Delta t$  is the time interval since the last event occurred at  $\mathbf{u}$ . To simplify the formulation, we omit position  $\mathbf{u}$  in the equations above.

However, event streams in low light often contain trailing artifacts [15, 17, 20] (Fig. 4(d)), which is not covered by the simplified modeling in Eqn. 1. To better model it, we revisit event generation process. As shown in Fig. 4 (a), the photodiode (PD) converts an incoming incident light to photocurrent, whose magnitude is effected by the cutoff frequency  $f_c$  of the camera system [17, 20] as

$$f_c = \frac{1}{2\pi C} \frac{I_{ph}}{U_t}, \quad (2)$$

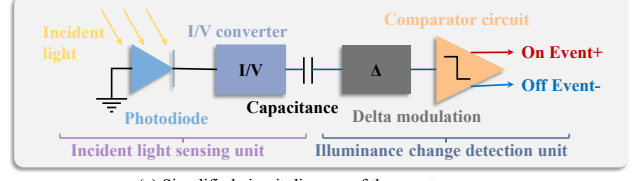
where  $C$  is the capacitance, and  $U_t$  is the thermal voltage. One can see that  $f_c$  is proportional to  $I_{ph}$ . Thus, the measured intensity or volume for event generation can be modeled as:

$$I'_t = \alpha I_t + (1 - \alpha) I_{t-\Delta t}, \quad (3)$$

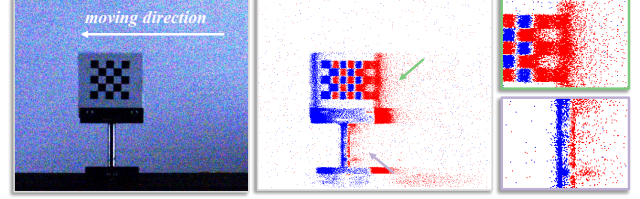
where  $\alpha = 1 - e^{-\Delta t/\tau}$  and  $\tau = 1/(2\pi f_c)$ . And thus we can approximately obtain the degraded event representation in the low light:

$$E_t = \begin{cases} 1, & \text{if } \log(\alpha I_t + (1 - \alpha) I_{t-\Delta t}) - \log(I_{t-\Delta t}) \geq c, \\ -1, & \text{if } \log(\alpha I_t + (1 - \alpha) I_{t-\Delta t}) - \log(I_{t-\Delta t}) \leq -c, \\ 0, & \text{otherwise.} \end{cases} \quad (4)$$

Equations above explain the cause of trailing. When image intensity decreases, the cutoff frequency also decreases (Eqn. 2), leading to a smaller value of  $\alpha$ . Consequently, the measurement of current intensity is more significantly influenced by prior values, an effect modeled as an RC low-pass filter [6, 17]. Such a configuration implies that the same voltage changes can induce more extended temporal delays in the generation of event signals in the low light condition. In Fig. 4(d), we display a real-world captured low-light event, where a temporal delay in the event data can be observed, leading to spatial trailing artifacts. Using such degraded event data for frame interpolation results in deformations in the interpolated frames due to the trailing effects (see Fig. 1).



(a) Simplified circuit diagram of the event camera



(b) Noisy RGB at 35lux

(c) Events at 35lux

(d) Trailing artifact

Figure 4. Simplified circuit diagram for each pixel of the event camera. And the visualization of event trailing artifacts, captured by our EVS-RGB beam splitting imaging system.

#### 3.2. Low Light Event-VFI

For common Event-VFI, the interpolation is modeled using Eqn. 1 and formulated as [9, 16, 27]:

$$I_{t+\Delta t} \approx I_t \cdot \exp \left( \int_t^{t+\Delta t} c \cdot E_\tau d\tau \right). \quad (5)$$

In low-light conditions, the event representation defined in Eqn. 4 accounts for temporal latency. When  $\Delta t$  is very small, the synthesis frames can be approximately modeled using the degraded event signals:

$$I_{t+\Delta t} \approx \frac{1}{\alpha} (I_t \cdot \exp \left( \int_t^{t+\Delta t} c \cdot E_\tau d\tau \right) - (1 - \alpha) I_t). \quad (6)$$

Compared with Eqn. 5, the low light Event-VFI needs to handle noisy RGB image  $I_t$  and consider the impact of trailing artifacts of events which is effect by  $\alpha$ .

In recent methods [11, 29, 30], to recover an intermediate RGB frame  $I_{t+\Delta t}$  between  $I_t$  and  $I_{t+1}$ , information from both the forward (from  $I_t$  to  $I_{t+\Delta t}$ ) and the backward (from  $I_{t+1}$  to  $I_{t+\Delta t}$ ) estimation are utilized. Thus process of low light Event-VFI in Eqn. 6 is solved as:

$$\hat{I}_{t+\Delta t} = \Phi(I_t, I_{t+1}, E_{t,t+\Delta t}, E_{t+\Delta t,t+1}, c, \alpha), \quad (7)$$

where  $\Phi$  is the interpolation.

Note that given that the threshold  $c$  and the latency factor  $\alpha$ , which are influenced by illuminance levels and camera hardware, adapting a pre-trained model to different conditions is challenging. Therefore, in Sec. 4.1, we will propose a per-scene optimization strategy specifically designed for the Event-VFI task, capable of addressing event latency across various camera settings.



## 4. Method

For the low light Event-VFI, the input are noisy low frame rate RGB images  $\{I_{t_k}\}_{k=1}^N$  together with the comprehensive event data  $E_{t_1 \rightarrow t_N}$ , where  $N$  denotes the sequence length. The objective of Event-VFI is to obtain the interpolated results  $I_{t+\Delta t}$  between two neighbor frames  $I_t$  and  $I_{t+1}$ , where  $\Delta t \in (t, t+1)$ . As illustrated in Eqn. 7, the interpolation in low-light conditions depends not only on the input frames  $I_t$  and  $I_{t+1}$ , events  $E_{t,t+1}$ , and threshold  $c$ , but also on the latency or trailing of the event signal  $\alpha$  in Eqn. 3.

Due to the trailing artifacts and other degradations in events that are difficult to be modeled at the training stage, we will introduce a per-scene optimization method in Sec. 4.1, with its associated loss function presented in Sec. 4.2. Moreover, to obtain a better per-trained model, we also present improvements to the low-light event simulation process in Sec. 4.3. The overall pipeline is summarized in Fig. 3.

### 4.1. Per-scene Optimization for VFI

Based on the insight that factors such as illuminance, camera hardware, and capture settings significantly influence event trailing and other degradations, and remain relatively constant within a single video, we propose per-scene optimization. This method allows the Event-VFI backbone to adapt to the current scene’s specific event degradation, enabling effective handling of Event VFI under low-light conditions with varying camera settings.

Unlike previous Event-VFI methods [14, 34], which rely solely on two consecutive noisy RGB frames and associated event signals to predict intermediate RGB frames, our per-scene optimization strategy leverages the entire sequence. This approach, depicted in Fig. 3, allows for fine-tuning a pre-trained Event-VFI model using the entire video sequence. It establishes training pairs directly from the testing sequence, using the denoised RGB image  $I_t$  at time  $t$  as the ground truth to supervise the interpolation results from two other captured RGB frames ( $I_{t-n}$  and  $I_{t+n}$ ) at neighboring timestamps, along with event signals ( $E_{t-n,t}$  and  $E_{t,t+n}$ ) captured during this interval, where  $n$  represents the temporal interval between captured RGB frames and is randomly sampled to enrich the data for per-scene optimization.

After per-scene fine-tuning, during the actual inference stage, the network utilizes the same sequence to generate a new frame  $\hat{I}_{t+\Delta t}$ , effectively increasing the frame rate.

### 4.2. Optimization Loss

In the per-scene optimization process, the interpolated frame at timestamp  $t$ ,  $\hat{I}_t$ , can be modeled as:

$$\hat{I}_t = \Phi(D(I_{t-n}), D(I_{t+n}), E_{t-n,t}, E_{t,t+n}), \quad (8)$$

where  $\Phi(\cdot)$  is the event-based frame interpolation network,  $D(\cdot)$  is the real-world denoising operator, and  $\lambda$  is a weight-

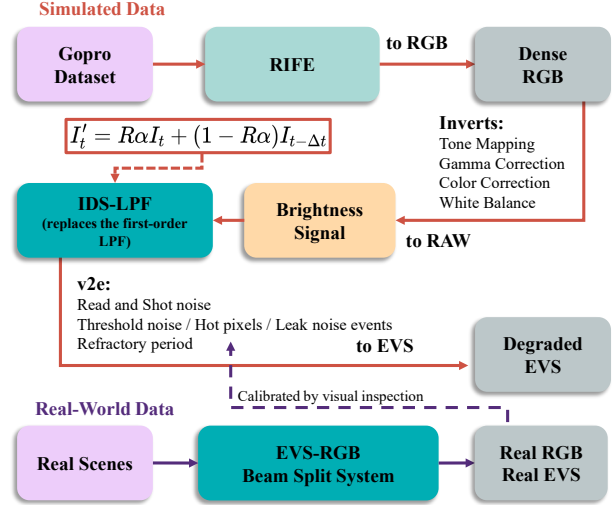


Figure 5. Synthesis process for the EVS motion trail simulation dataset.

ing parameter which we set to 0.1. In our experiment, we choose state-of-the-art Event-VFI model TimeLens [30] as interpolation backbone  $\Phi(\cdot)$  and Restormer [31] as denoiser  $D(\cdot)$ . Then the reconstruction loss can be defined as:

$$\mathcal{L}_r = \sqrt{\|\hat{I}_t - D(I_t)\|^2 + \epsilon^2} + \lambda \sqrt{\|S(\hat{I}_t) - S(D(I_t))\|^2 + \epsilon^2}, \quad (9)$$

where  $\lambda$  is set as 0.1,  $S(\cdot)$  is the Sobel operator,  $\sqrt{\|\hat{x} - x\|^2 + \epsilon^2}$  is the Charbonnier penalty function, and  $\epsilon$  is set to 0.001. Additionally, to obtain visually pleasing interpolation results, the perceptual loss [10] is also used:

$$\mathcal{L}_p = \beta \sqrt{\|\text{VGG}(\hat{I}_t) - \text{VGG}(D(I_t))\|^2 + \epsilon^2}, \quad (10)$$

where  $\text{VGG}(\cdot)$  is the pretrained 16 layer VGG network [23],  $\beta$  is a weighting parameter which we set to 0.1.

### 4.3. Low Light Event Simulation

In this sub-section, we also discuss how to improve the pretrained interpolation model using a more accurate event simulation pipeline. Even with the per-scene optimization proposed above, a robust pretrained model is still critical, as it helps to reduce tuning time and improve performance after per-scene optimization.

Fig. 5 shows the proposed simulation pipeline. First, we create a high-frame linear RGB sequences using the GoPro dataset [32]. Initially, we employ RIFE [7] to generate high frame rate video. Subsequently, we compute a low light intensity image using  $L = \Gamma^{-1}(I)$ , where  $\Gamma^{-1}(\cdot)$  represents the inverse of the image signal processing (ISP) pipeline. In applying  $\Gamma^{-1}(\cdot)$ , we follow [3] and incorporate inverse

tone mapping, inverse gamma correction, inverse color correction matrix, and inverse white balance and brightening to transition the data to a linear brightness domain.

In the second step, to create events from high-frame-rate linear RGB sequences, we use v2e simulator to produce a synthetic RGB-EVS dataset. Under low-light conditions, the degradation of event cameras can generally be attributed to motion trails and noise. The v2e [6] simulator comprehensively models noise factors through parameter adjustments, such as threshold noise, hot pixels, leak noise events, and refractory period violations. To more accurately simulate motion trailing associated with events, we employ a second-order low-pass filter to approximate the RC circuit dynamics described in Eqn. 3 of Sec. 3.1.

In the last step, we further improve the quality of generated event signals. Even we increase the input video frame rate using RIFE interpolation method, the resulting video is still a temporal discretization of the event signal. Event signals often occur randomly within brief intervals between frames. To mitigate this issue, we have refined the low-pass filter approach by incorporating a sparse event mask  $R$  that resets certain event pixels  $I_{t-\Delta t}$  to zero, allowing these pixels to respond exclusively to instantaneous light intensity changes in the current frame. This adjustment helps induce sparsity in the event tails, better approximating real-world scenarios. Consequently, we reformulate the low-pass filter equation in Eqn. 3 as follows:

$$I'_t = R\alpha I_t + (1 - R\alpha)I_{t-\Delta t}, \quad (11)$$

where  $R$  is a random binary mask,  $\alpha$  is the event trailing factor as shown in Eqn. 3. The event-RGB data pairs generated from this modified filter are utilized to pretrain the frame interpolation model. By employing the designed simulation pipeline, our method achieves superior results compared to the original TimeLens, as demonstrated in Tab. 1 in low light Event-VFI.

## 5. Experiments

### 5.1. Experiment Details

We selected the state-of-the-art TimeLens [30] as the backbone for our Event-VFI model. Initially, a model tailored for low-light Event-VFI, referred to as Our Pretrained, is trained using simulated data (as detailed in Sec. 4.3). Before inference phase for each scene, per-scene optimization is first performed using the Adam optimizer [12] with a learning rate of  $1 \times 10^{-4}$ . The optimized model is denoted as Our Per Scene Opt. It is important to note that to simplify the learning process, we pre-denoise the input RGB images using Restormer [31].

Our method is compared with last RGB-VFI techniques (SuperSloMo [8] and RIFE [7]) and state-of-the-art Event-VFI methods (CBMNet [11] and TimeLens [30]).

### 5.2. Low Light Event-VFI Benchmark: EVFI-LL

Previous real-world Event-VFI datasets, *i.e.*, BS-ERGB [30] and ERF-X170FPS [11], were captured under normal lighting conditions and are not suitable for testing the trailing artifacts in low light events. Therefore, we have captured a new low-light Event-VFI benchmark, denoted as EVFI-LL.

Similar to ERF-X170FPS [11], our setup employs a beam splitter to align the fields of view of the event and RGB cameras, as depicted in Fig. 6. We use a Prophesee EVK4-HD (1280 × 720) event camera and a MER2-301-125U3C (2048 × 1536) RGB camera. Our system ensures that both cameras are geometrically calibrated and temporally synchronized. Calibration is achieved by estimating transformations using a blinking checkerboard pattern, and synchronization is managed with synchronization trigger controls.

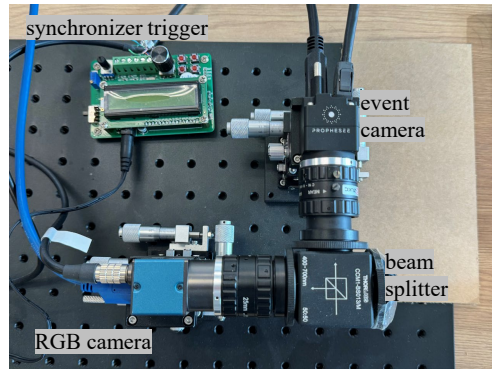


Figure 6. EVS-RGB beam splitting imaging system. Spatial-temporal alignment is ensured through calibration and trigger control.

To capture the low-light Event-RGB dataset, we set the ambient light level to below 35 Lux and used short exposure times to minimize blur. The dataset includes 10 non-linear motion scenarios, such as rotating balls and twisting paper sheets. To test the generalization capability of various methods, we captured additional sequences with varying camera parameters, particularly ON/OFF thresholds. During data acquisition, the RGB camera’s frame rate was maintained at 64Hz.

For testing purposes, we subsampled the test video by skipping every N-1 frames, which resulted in an effective testing frame rate reduced by a factor of N. Event data is not skipped during testing. This lower frame rate poses a significant challenge for frame interpolation tasks, using the skipped frames as ground truth for performance evaluation. We also curated more challenging scenes with complex and large motions within the EVFI-LL dataset, creating a challenging track denoted as EVFI-LL-C.

Table 1. Comparison of different frame interpolation methods on EVFI-LL under various interpolation rates (4× and 8×) and different bias voltages. The lower the bias, the lower the threshold, the more events recorded. The Sony IMX636 sensor in the Prophesee EVK4-HD event camera has positive and negative threshold voltages biased to 0 by default.

Bias Setting	Method	4× Frame Interpolation			8× Frame Interpolation		
		PSNR ↑	SSIM ↑	LPIPS ↓	PSNR ↑	SSIM ↑	LPIPS ↓
+20	SuperSloMo [8]	30.201	0.8802	0.1371	27.665	0.8559	0.1828
	RIFE [7]	31.143	0.8846	0.1420	28.523	0.8642	0.1854
	TimeLens [30]	30.548	0.8673	0.1691	29.187	0.8559	0.1887
	CBMNet [11]	30.114	0.8592	0.1999	28.656	0.8465	0.2246
	Our Pretrained	30.803	0.8805	0.1522	29.449	0.8698	0.1708
	Our Per Scene Opt.	<b>31.442</b>	<b>0.8848</b>	<b>0.1285</b>	<b>30.760</b>	<b>0.8795</b>	<b>0.1381</b>
0	SuperSloMo [8]	31.105	0.8857	0.1264	28.724	0.8626	0.1632
	RIFE [7]	32.242	0.8901	0.1301	29.462	0.8687	0.1706
	TimeLens [30]	30.729	0.8647	0.1584	29.891	0.8542	0.1728
	CBMNet [11]	30.323	0.8662	0.1878	29.320	0.8552	0.2100
	Our Pretrained	31.218	0.8836	0.1380	30.338	0.8730	0.1505
	Our Per Scene Opt.	<b>32.762</b>	<b>0.8972</b>	<b>0.1172</b>	<b>32.135</b>	<b>0.8879</b>	<b>0.1215</b>
-20	SuperSloMo [8]	30.980	0.8880	0.1269	28.912	0.8683	0.1648
	RIFE [7]	32.061	0.8920	0.1307	29.702	0.8744	0.1689
	TimeLens [30]	31.417	0.8743	0.1572	30.541	0.8662	0.1706
	CBMNet [11]	30.838	0.8607	0.1892	29.814	0.8509	0.2120
	Our Pretrained	32.036	0.8915	0.1329	31.241	0.8835	0.1431
	Our Per Scene Opt.	<b>32.990</b>	<b>0.8977</b>	<b>0.1073</b>	<b>32.529</b>	<b>0.8913</b>	<b>0.1170</b>

### 5.3. Results on Real-world Low-Light Event-VFI

We evaluated methods on EVFI-LL dataset at 4× and 8× interpolation rates across various event triggering thresholds. The quantitative results are presented in Tab. 1. For evaluation, we employed both numerical metrics, such as PSNR and SSIM, and the perceptual metric, LPIPS [33]. We also conducted evaluations on the challenging track, EVFI-LL-C, with quantitative comparisons detailed in Tab. 2. Visual comparisons are shown in Fig. 7.

In Tabs. 1 and 2, one interesting observation is that when the interpolated ratio is small (4×), event-based methods (TimeLens and CBMNet) even perform worse than RGB-only methods (SuperSloMo and RIFE). This is because the degradation of the low-light event signal and the domain gap between training and testing significantly hurt the performance of event-based solution. Still, in more challenging 8× interpolation, the Event-VFI methods performs better than RGB-VFI methods, because the additional event stream does provide more information about intermediate motion. Despite this, as shown in Fig. 7, the previous methods fail to account for the trailing artifacts of low-light events, leading to visually displeasing interpolated results with noticeable deformations around object edges.

In contrast, benefiting from per-scene optimization, our

Table 2. Comparison of different frame interpolation methods in challenging track in EVFI-LL-C with 8× interpolation rates.

Method	PSNR ↑	SSIM ↑	LPIPS ↓
SuperSloMo [8]	26.269	0.8039	0.2341
RIFE [7]	26.668	0.8122	0.2437
TimeLens [30]	30.945	0.8401	0.1818
CBMNet [11]	30.552	0.8431	0.2357
Our Pretrained	31.471	0.8543	0.1532
Our Per Scene Opt.	<b>31.948</b>	<b>0.8695</b>	<b>0.1472</b>

enhanced model, Our Per Scene Opt., consistently outperforms the previous methods across all interpolation scales and bias settings. Notably, our model achieves nearly a 2dB improvement on the entire EVFI-LL dataset compared to the second-best methods. As depicted in Fig. 7, our per-scene optimized results preserve crisp details and textures while accurately rendering motions.

## 6. Discussion

**Low light simulation pipeline.** In Tab. 3, it is evident that Our Pretrained (TimeLens) achieves an improvement of 0.5



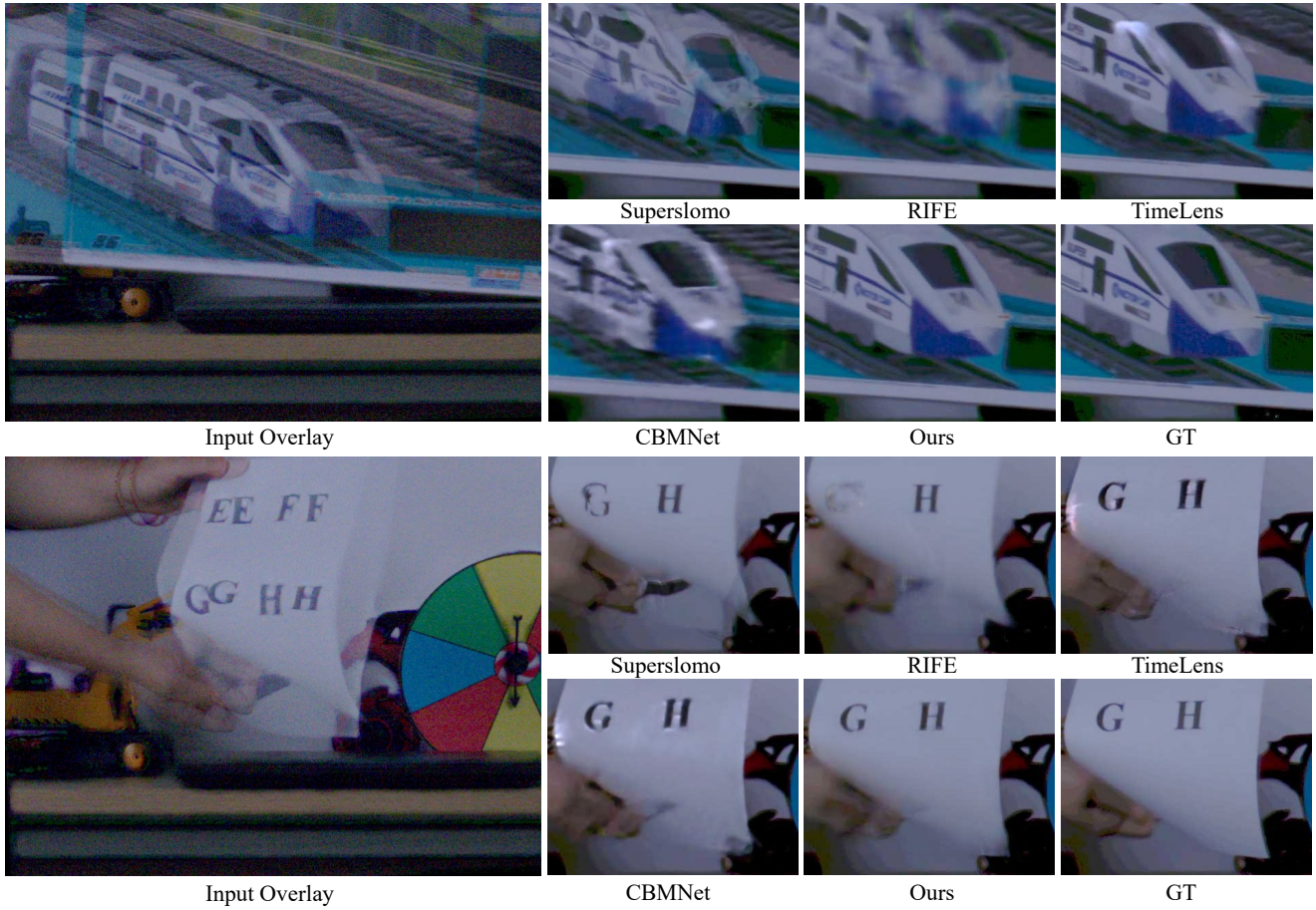


Figure 7. Visual comparison of results from different methods under large motion.

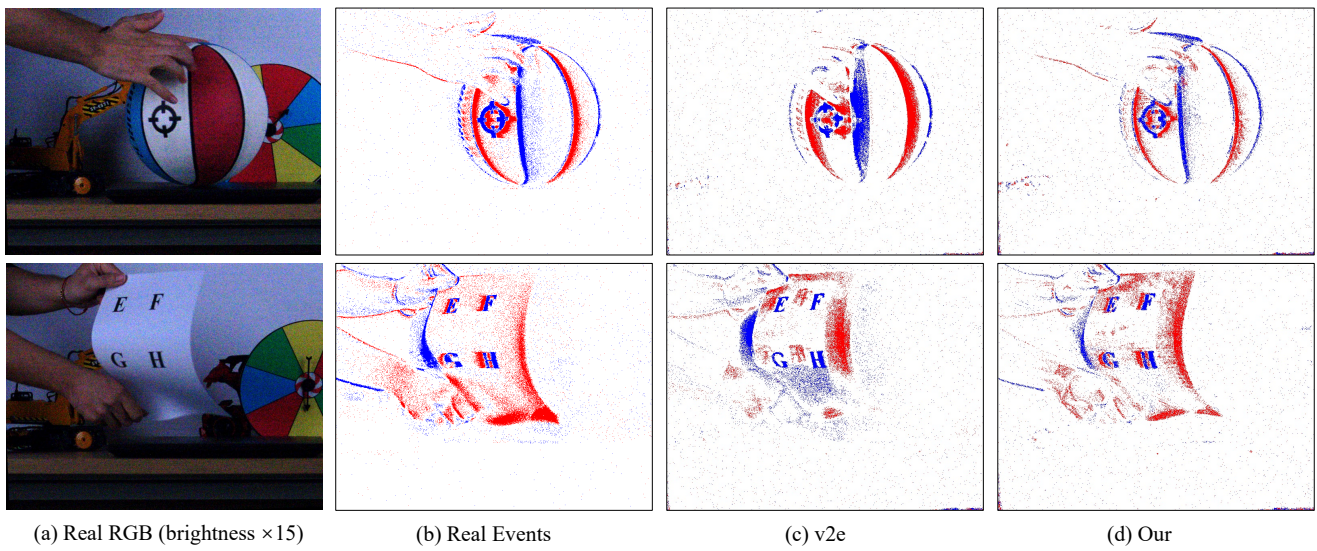


Figure 8. Visual comparison of the low-light trailing simulation results of the event camera with v2e[6].



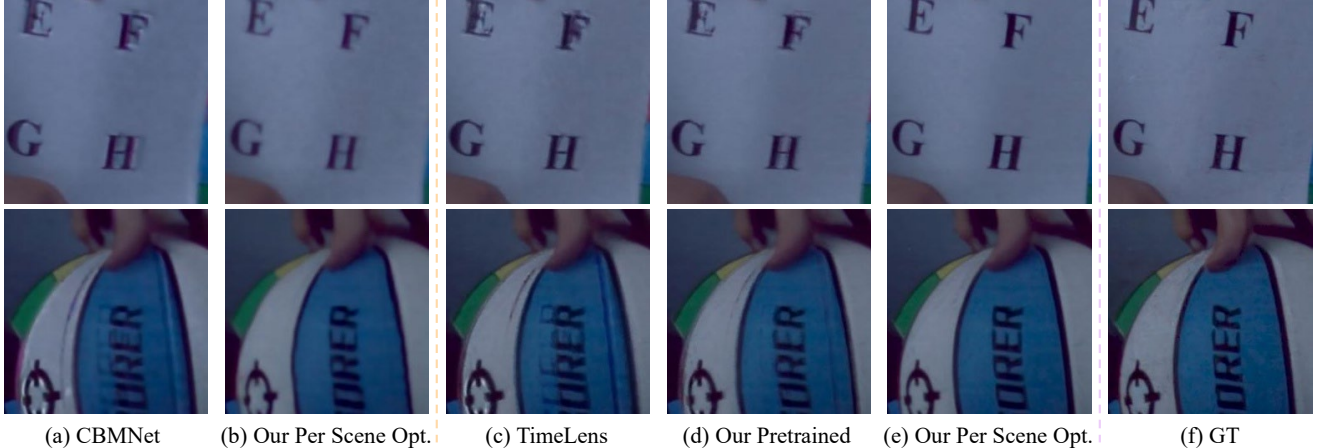


Figure 9. Visual comparison of ablation study results.

to 1 dB over the original TimeLens under low-light conditions, demonstrating the effectiveness of our simulation pipeline. Fig. 8 offers visual comparisons of our simulation with typical v2e simulation[6]. The visualizations distinctly show the sparse and asymmetric event patterns, which are characteristic of low-light conditions and the fundamental operating principles of event cameras. Unlike merely adjusting the parameters of the v2e simulator, our method synthesizes event representations that convincingly mimic real sensor data, including accurate depictions of the elongated event streaks caused by latency.

**Per-scene optimization.** We propose a per-scene optimization strategy to address the challenges of Event-VFI under low-light conditions. By creating supervision pairs directly from the test sequence, the Event-VFI network can be optimized to incrementally adapt to the current scene’s specific event degradation. Our experimental results, detailed in Tab. 3, show that our per-scene optimization strategy, *Our Per Scene Opt. (TimeLens)*, significantly enhances interpolation quality under real-world low-light conditions compared to the unoptimized model, *Our Pretrained (TimeLens)*. As illustrated in Fig. 1, the optimized outcomes reveal sharply recovered motion details, and observe no ghosting or trailing artifacts.

**Running time of per-scene optimization.** We conducted a comparative analysis of the running times for the per-scene optimization stage and the inference stage on an NVIDIA RTX 4090. Given that the optimization process encompasses data loading durations, we calculated the total runtime of the whole program. For the configuration where eight frames are interpolated between two images of size  $736 \times 576$ , TimeLens exhibited an approximate average runtime of 0.16 seconds, whereas the per-scene optimization process required about average 0.22 seconds. Notably, even though our method incorporates a training com-

Table 3. Ablation Study on  $\times 8$  Frame Interpolation on EVFI-LL

Method	PSNR $\uparrow$	SSIM $\uparrow$	LPIPS $\downarrow$
CBMNet	29.265	0.8509	0.2155
Our Per Scene Opt. (CBMNet)	31.012	0.8899	0.2101
TimeLens	29.873	0.8588	0.1774
Our Pretrained (TimeLens)	30.343	0.8754	0.1548
Our Per Scene Opt. (TimeLens)	31.808	0.8862	0.1256

ponent, the time taken for per-scene optimization is significantly less than the time required for training from scratch, which takes approximately three days to train models like Our Pretrained (TimeLens). The duration of the per-scene optimization is roughly on the same order of magnitude as the inference time.

**Generalize to other backbones.** To demonstrate the generalizability of per-scene optimization across different backbones, we also applied such strategy to CBMNet. As shown in Tab. 3, Our Per Scene Opt. (CBMNet) exhibited a performance enhancement of  $\sim 1.8$  dB in low-light conditions. The visual comparison in Fig. 9 evident that the Our Per Scene Opt. (CBMNet) effectively reduces the impact of event trailing artifacts, yielding visually pleasing results. This improvement underscores the potential of per-scene optimization to significantly enhance the generalizability of other Event-VFI algorithms. Additionally, since the original CBMNet model was not trained considering low-light trailing effects, the performance of Our Per Scene Opt. (CBMNet) were somewhat inferior to those achieved with Our Per Scene Opt. (TimeLens), highlighting the importance of a well-pretrained model.

## 7. Conclusion

In conclusion, this study introduced a novel approach to address the challenges inherent in event-based video frame interpolation (Event-VFI) under low-light conditions. Trailing artifacts and other signal degradations present in low-light event data are difficult to accurately model during the training phase. To tackle these issues, we have developed a per-scene optimization strategy tailored for general Event-VFI applications in low-light environments. Empirical evidence demonstrates that our per-scene optimization significantly enhances the generalizability of Event-VFI algorithms in low-light scenarios. This optimization effectively mitigates artifacts caused by event trailing and reduces errors in the interpolated frame positions. Furthermore, to evaluate Event-VFI methods in low-light condition, this study collected the EVFI-LL dataset, specifically tailored for low-light environments and varying event camera settings, further underscores our contribution by providing a robust platform for testing and benchmarking low light Event-VFI algorithms.

**Limitations.** The proposed method currently also has several limitations, which we aim to address in future work. First, the current optimization approach does not account for the impact of blur. Although the existing Event-VFI datasets significantly reduce blur by lowering exposure times, this constraint limits the applicability of the algorithm in broader scenarios. Second, similar to previous works, our datasets have been collected using only a single model of event camera. In the future, we hope to further validate the generalizability of our algorithm across different devices.

## References

- [1] Wenbo Bao, Wei-Sheng Lai, Chao Ma, Xiaoyun Zhang, Zhiyong Gao, and Ming-Hsuan Yang. Depth-aware video frame interpolation. In *Proceedings of the IEEE/CVF conference on computer vision and pattern recognition*, pages 3703–3712, 2019. 1, 2, 3
- [2] Christian Brandli, Raphael Berner, Minhao Yang, Shih-Chii Liu, and Tobi Delbruck. A 240×180 130 db 3 us latency global shutter spatiotemporal vision sensor. *IEEE Journal of Solid-State Circuits*, 49(10):2333–2341, 2014. 1
- [3] Tim Brooks, Ben Mildenhall, Tianfan Xue, Jiawen Chen, Dillon Sharlet, and Jonathan T Barron. Unprocessing images for learned raw denoising. In *Proceedings of the IEEE/CVF conference on computer vision and pattern recognition*, pages 11036–11045, 2019. 5
- [4] Rui Graça and Tobi Delbruck. Unraveling the paradox of intensity-dependent dvs pixel noise. *arXiv preprint arXiv:2109.08640*, 2021. 2
- [5] Rui Graça, Brian McReynolds, and Tobi Delbruck. Shining light on the dvs pixel: A tutorial and discussion about biasing and optimization. In *Proceedings of the IEEE/CVF Conference on Computer Vision and Pattern Recognition*, pages 4044–4052, 2023. 2
- [6] Yuhuang Hu, Shih-Chii Liu, and Tobi Delbruck. v2e: From video frames to realistic dvs events. In *Proceedings of the IEEE/CVF Conference on Computer Vision and Pattern Recognition*, pages 1312–1321, 2021. 2, 3, 4, 6, 8, 9
- [7] Zhewei Huang, Tianyuan Zhang, Wen Heng, Boxin Shi, and Shuchang Zhou. Real-time intermediate flow estimation for video frame interpolation. In *European Conference on Computer Vision*, pages 624–642. Springer, 2022. 1, 2, 3, 5, 6, 7
- [8] Huaizu Jiang, Deqing Sun, Varun Jampani, Ming-Hsuan Yang, Erik Learned-Miller, and Jan Kautz. Super slo-mo: High quality estimation of multiple intermediate frames for video interpolation. In *Proceedings of the IEEE conference on computer vision and pattern recognition*, pages 9000–9008, 2018. 6, 7
- [9] Zhe Jiang, Yu Zhang, Dongqing Zou, Jimmy Ren, Jiancheng Lv, and Yebin Liu. Learning event-based motion deblurring. In *CVPR*, pages 3320–3329, 2020. 4
- [10] Justin Johnson, Alexandre Alahi, and Li Fei-Fei. Perceptual losses for real-time style transfer and super-resolution. In *Eur. Conf. Comput. Vis.*, pages 694–711. Springer, 2016. 5
- [11] Taewoo Kim, Yujeong Chae, Hyun-Kurl Jang, and Kuk-Jin Yoon. Event-based video frame interpolation with cross-modal asymmetric bidirectional motion fields. In *Proceedings of the IEEE/CVF Conference on Computer Vision and Pattern Recognition*, pages 18032–18042, 2023. 1, 2, 3, 4, 6, 7
- [12] Diederik P Kingma and Jimmy Ba. Adam: A method for stochastic optimization. *arXiv preprint arXiv:1412.6980*, 2014. 6
- [13] Guoqiang Liang, Kanghao Chen, Hangyu Li, Yunfan Lu, and Lin Wang. Towards robust event-guided low-light image enhancement: A large-scale real-world event-image dataset and novel approach. *arXiv preprint arXiv:2404.00834*, 2024. 2
- [14] Jinxiu Liang, Yixin Yang, Boyu Li, Peiqi Duan, Yong Xu, and Boxin Shi. Coherent event guided low-light video enhancement. In *Proceedings of the IEEE/CVF International Conference on Computer Vision*, pages 10615–10625, 2023. 2, 3, 5
- [15] Patrick Lichtsteiner, Christoph Posch, and Tobi Delbruck. A 128x128 120 db 15us latency asynchronous temporal contrast vision sensor. *IEEE journal of solid-state circuits*, 43(2):566–576, 2008. 1, 3, 4
- [16] Songnan Lin, Jiawei Zhang, Jinshan Pan, Zhe Jiang, Dongqing Zou, Yongtian Wang, Jing Chen, and Jimmy Ren. Learning event-driven video deblurring and interpolation. In *ECCV*, pages 695–710. Springer, 2020. 4
- [17] Haoyue Liu, Shihan Peng, Lin Zhu, Yi Chang, Hanyu Zhou, and Luxin Yan. Seeing motion at nighttime with an event camera. *arXiv preprint arXiv:2404.11884*, 2024. 1, 2, 3, 4
- [18] Simone Meyer, Abdelaziz Djelouah, Brian McWilliams, Alexander Sorkine-Hornung, Markus Gross, and Christopher Schroers. Phasenet for video frame interpolation. In *Proceedings of the IEEE Conference on Computer Vision and Pattern Recognition*, pages 498–507, 2018. 2
- [19] Simon Niklaus, Long Mai, and Feng Liu. Video frame in-

- terpolation via adaptive separable convolution. In *Proceedings of the IEEE international conference on computer vision*, pages 261–270, 2017. [2](#)
- [20] Christoph Posch, Daniel Matolin, and Rainer Wohlgenannt. A qvga 143 db dynamic range frame-free pwm image sensor with lossless pixel-level video compression and time-domain cds. *IEEE Journal of Solid-State Circuits*, 46(1):259–275, 2010. [1](#), [2](#), [3](#), [4](#)
- [21] Henri Rebecq, Daniel Gehrig, and Davide Scaramuzza. Esim: an open event camera simulator. In *Conference on robot learning*, pages 969–982. PMLR, 2018. [2](#), [3](#)
- [22] Antonio Rios-Navarro, Shasha Guo, Abarajithan Gnaneswaran, Keerthivasan Vijayakumar, Alejandro Linares-Barranco, Thea Aarrestad, Ryan Kastner, and Tobi Delbruck. Within-camera multilayer perceptron dvs denoising. In *Proceedings of the IEEE/CVF Conference on Computer Vision and Pattern Recognition*, pages 3932–3941, 2023. [2](#)
- [23] Olga Russakovsky, Jia Deng, Hao Su, Jonathan Krause, Sanjeev Satheesh, Sean Ma, Zhiheng Huang, Andrej Karpathy, Aditya Khosla, Michael Bernstein, et al. Imagenet large scale visual recognition challenge. *International journal of computer vision*, 115:211–252, 2015. [5](#)
- [24] Teresa Serrano-Gotarredona and Bernabé Linares-Barranco. A 128×128 1.5% contrast sensitivity 0.9% fpn 3us latency 4 mw asynchronous frame-free dynamic vision sensor using transimpedance preamplifiers. *IEEE Journal of Solid-State Circuits*, 48(3):827–838, 2013. [1](#)
- [25] Zhihao Shi, Xiangyu Xu, Xiaohong Liu, Jun Chen, and Ming-Hsuan Yang. Video frame interpolation transformer. In *Proceedings of the IEEE/CVF Conference on Computer Vision and Pattern Recognition*, pages 17482–17491, 2022. [2](#)
- [26] Hyeonjun Sim, Jihyong Oh, and Munchurl Kim. Xvfi: extreme video frame interpolation. In *Proceedings of the IEEE/CVF international conference on computer vision*, pages 14489–14498, 2021. [1](#), [2](#), [3](#)
- [27] Lei Sun, Christos Sakaridis, Jingyun Liang, Qi Jiang, Kailun Yang, Peng Sun, Yaozu Ye, Kaiwei Wang, and Luc Van Gool. Event-based fusion for motion deblurring with cross-modal attention. In *ECCV*, pages 412–428. Springer, 2022. [4](#)
- [28] Lei Sun, Christos Sakaridis, Jingyun Liang, Peng Sun, Jiezhong Cao, Kai Zhang, Qi Jiang, Kaiwei Wang, and Luc Van Gool. Event-based frame interpolation with ad-hoc deblurring. In *Proceedings of the IEEE/CVF Conference on Computer Vision and Pattern Recognition*, pages 18043–18052, 2023. [1](#), [3](#)
- [29] Stepan Tulyakov, Alfredo Bochicchio, Daniel Gehrig, Stamatios Georgoulis, Yuanyou Li, and Davide Scaramuzza. Time lens++: Event-based frame interpolation with parametric non-linear flow and multi-scale fusion. In *Proceedings of the IEEE/CVF Conference on Computer Vision and Pattern Recognition*, pages 17755–17764, 2022. [2](#), [3](#), [4](#)
- [30] Stepan Tulyakov, Daniel Gehrig, Stamatios Georgoulis, Julius Erbach, Mathias Gehrig, Yuanyou Li, and Davide Scaramuzza. Time lens: Event-based video frame interpolation. In *Proceedings of the IEEE/CVF conference on computer vision and pattern recognition*, pages 16155–16164, 2021. [1](#), [2](#), [3](#), [4](#), [5](#), [6](#), [7](#)
- [31] Syed Waqas Zamir, Aditya Arora, Salman Khan, Munawar Hayat, Fahad Shahbaz Khan, and Ming-Hsuan Yang. Restormer: Efficient transformer for high-resolution image restoration. In *IEEE Conf. Comput. Vis. Pattern Recog.*, pages 5728–5739, 2022. [5](#), [6](#)
- [32] Richard Zhang, Phillip Isola, Alexei A Efros, Eli Shechtman, and Oliver Wang. The unreasonable effectiveness of deep features as a perceptual metric. In *CVPR*, pages 586–595, 2018. [5](#)
- [33] Richard Zhang, Phillip Isola, Alexei A Efros, Eli Shechtman, and Oliver Wang. The unreasonable effectiveness of deep features as a perceptual metric. In *CVPR*, 2018. [7](#)
- [34] Chu Zhou, Minggui Teng, Jin Han, Jinxiu Liang, Chao Xu, Gang Cao, and Boxin Shi. Deblurring low-light images with events. *International Journal of Computer Vision*, 131(5):1284–1298, 2023. [2](#), [3](#), [5](#)